ELSEVIER

Vaccine 18 (2000) 362–370

Vaccine

www.elsevier.com/locate/vaccine

Surface plasmon resonance screening of synthetic peptides mimicking the immunodominant region of C-S8c1 foot-and-mouth disease virus

Paula Gomes, Ernest Giralt, David Andreu*

Department of Organic Chemistry, University of Barcelona, Martí i Franquès, 1; 08028 Barcelona, Spain

Abstract

The main antigenic site (site A) of foot-and-mouth disease virus (FMDV, strain C-S8c1) may be adequately reproduced by a 15-peptide with the amino acid sequence H-YTASARGDLAHLTTT-NH_2 (A15), corresponding to the residues 136–150 of the viral protein VP1. The effect of amino acid substitutions within A15 on its antigenicity towards monoclonal antibodies (MAb) raised against antigenic site A, has been studied by means of BIAcore technology, based on surface plasmon resonance (SPR). Although these antigenicities have previously been determined from enzyme-linked immunosorbent assays (ELISA), the SPR-based technique is superior in that it allows a fast and straightforward screening of antigens while simultaneously providing kinetic data of the antigen–antibody interaction. With a view to screening fairly large libraries of individual peptides, we have inverted the typical SPR experiment by immobilizing the MAb on the sensor surface and using peptides as soluble analytes. We report the validation of this approach through the screening of 44 site A peptides, with results generally in good agreement with the relative antigenicities previously determined by competition ELISA.

Keywords: Biosensor; small peptide analytes; Foot-and-mouth disease virus

1. Introduction

The study of biospecific macromolecular interactions is central to an understanding of the molecular mechanisms involved in viral infection and may help in the rational design of synthetic vaccines. The antigen–antibody reaction involves a series of molecular events that can be analyzed by different biophysical methods to provide qualitative or quantitative data on the binding reaction. Optical spectroscopies, particularly those based on fluorescence, have been widely employed so far, but with the introduction of surface plasmon resonance (SPR) in the early '90s, optical evanescent wave biosensors have become increasingly popular for characterization of reversible biospecific reactions [1–9]. SPR is an optical detection method that allows to monitor macromolecular interactions directly, in real-time and in a label-free mode, in contrast with indirect methods such as enzyme-linked immunosorbent assays (ELISA) or fluorescence spectroscopies requiring suitable tags. In addition, the ability to provide a real-time analysis means that not only affinity data but also kinetic data can be obtained. Another attractive feature is that high purity or large amounts of the biomolecules are not strictly required [1,7–10]. The technique relies on the covalent immobilization of one interactant (the ligand) onto a modified dextran-coated gold surface, which forms one wall of a flowcell [11,12]. A solution of the other interactant (the ligate or analyte) is injected over this surface at continuous flow. Monochromatic *p*-polarized light is directed at the sensor surface and biomolecular binding events are detected as changes in the specific angle where SPR creates extinction of light [1,7]. These changes reflect refractive index changes in the solution close to the

* Corresponding author. Tel.: +34-93-402-1260; fax: +34-93-402-1260.
E-mail address: andreu@admin.qo.ub.es (D. Andreu)

0264-410X/99/$ - see front matter
PII: S0264-410X(99)00206-6

Nomenclature

FMDV	foot-and-mouth disease virus
SPR	surface plasmon resonance
ELISA	enzyme-linked immunosorbent assay
MAb	monoclonal antibody
NHS	*N*-hydroxysuccinimide
EDC	*N*-ethyl-*N*′-dimethylaminopropylcarbodiimide
RU	resonance units
k_s	apparent kinetic rate constant
k_a	association kinetic rate constant
k_d	dissociation kinetic rate constant
R	biosensor response (in RU) at a given time
R_{max}	maximum response (in RU) for a given surface capacity
R_{immob}	ligand immobilization response
R_{eq}	extrapolated response (in RU) for the equilibrium
A	analyte
L	ligand
C_A	analyte concentration
K_A	association equilibrium constant
χ^2	chi squared
MW	molecular weight

surface, caused by the increase/decrease of mass due to analyte association/dissociation to the immobilized ligand. Therefore, measuring continuously the SPR angle provides a full record (a sensorgram) of the progress of the biospecific interaction.

Our research has been focused for some time on synthetic peptide vaccines against foot-and-mouth disease virus (FMDV), which causes the economically most important disease of cattle [13–18]. The high genetic variability of FMDV is responsible for the antigenic diversity among FMDV isolates and even within isolate subpopulations [13,16–19]. This fact is an important obstacle in the design of effective synthetic epitope-based vaccines. Ideally, such vaccines should include multiple epitopes to prevent the selection of resistant mutants in the field, and the effects of amino acid substitutions in infection-involved epitopes should be well characterized at the molecular level. We have directed our attention to the various overlapping linear B-cell epitopes within antigenic site A [13–15,17], located on the G–H loop of FMDV. This site can be adequately reproduced by peptide A15 (H-YTASARGDLAHLTTT-NH_2), corresponding to residues 136–150 of viral protein VP1. We have previously described the effect of systematic single-residue changes on the antigenicity of site A [18]. Since we wished to characterize these antigenic responses not only at equilibrium but also in kinetic terms, SPR was the method of choice. However, given the large number of variant peptides, the only practical way to perform the screening consists of monoclonal antibody (MAb) immobilization and injection of peptide analytes. As direct detection of analytes smaller than 5000 Da is usually unfeasible with standard BIAcore protocols [20,21], we have carried out an extensive optimization of this approach using 44 of the 240 A15 single mutants as analytes and anti-site A MAb SD6 as ligand. The generally good agreement found between biosensor data and the affinities known from ELISA [18] validates our analytical method.

2. Experimental procedures

2.1. Materials

MAb SD6 stock solution (1.6 mg/ml in PBS, pH 7.3) was obtained as described [14] by Dra. Nuria Verdaguer (CSIC, Barcelona). The antibody was desalted and buffer-exchanged on Nap-5 Sephadex G-25 columns (Pharmacia) and the eluate quantitated by the Pierce BCA protein assay method (Pierce). The synthesis and purification of A15 analogues has been previously described [18]. Consumables for the BIAcore 1000 instrument (CM5 certified sensor chips, HBS buffer, the amine coupling reagents *N*-hydroxysuccinimide (NHS) and *N*-ethyl-*N*′-dimethylaminopropyl-carbodiimide (EDC), ethanolamine) as well as the BIAevaluation 3.0.1 software were all from Biosensor AB (Uppsala, Sweden).

2.2. Biosensor experiments

2.2.1. M_{ab} pre-concentration and immobilization

SD6 solutions (100 and 50 μg/ml, in either 10 mM acetate, pH 5.0 or 5 mM maleate, pH 6.0) were separately injected (30 μl) at 5 μl/min over a non-activated sensor surface in order to determine which gave the most efficient pre-concentration of Mab into the dextran matrix. Three SD6 surfaces were prepared using the standard amine coupling procedure as described by the manufacturer. Each carboxymethyl surface was activated with a 35 μl injection (at 5 μl/min) of a NHS/EDC mixture and SD6 was then coupled at three different densities by exposing each surface to 35 μl injections of SD6 in 10 mM acetate buffer pH 5.0 at concentrations of 50, 5 and 3 μg/ml, respectively.

Unreacted activated groups were blocked by a 30 μl injection of ethanolamine and remaining non-covalently bound molecules were washed off in a regeneration step with a 3-min pulse of 100 mM HCl. The final densities of immobilized SD6 were 8000, 1700 and 800 RU, respectively (1000 RU corresponding to a 1 ng/mm^2 surface density).

2.2.2. Optimization of the experimental parameters

A few sets of experiments, using A15 as analyte, were run on the three SD6 surfaces at different peptide concentrations (ranging from 1 to 2440 nM) and flow rates (5 and 60 μl/min). A 2.44 mM solution of peptide in 100 mM acetic acid was used as stock, from which assay samples were prepared by 1000-fold and subsequent serial dilutions in HBS. All experiments were done in HBS running buffer at 25°C, using the 'kinjection' mode in order to obtain accurate kinetic data by decreasing sample dispersion at the injection plugs. To generate the sensorgrams peptide injections during 7 min followed by 6 min of dissociation in running buffer were used, prior to the regeneration cycle (2-min pulse with 100 mM HCl).

2.2.3. Kinetic analysis of A15 analogues

Once suitable experimental conditions for kinetic screening of site A peptides had been established (see Section 4), a systematic analysis of 43 A15 analogues was performed, in order to compare biosensor kinetic data with affinities previously determined by competition ELISA. This analysis was done on a medium density SD6 surface (1700 RU of immobilized MAb), at peptide concentrations ranging from ca. 2500 to 150 nM. Stock peptide solutions were quantitated by amino acid analysis. Sensorgrams were generated at a 60 μl/min flow rate and 'kinjections' consisted on a 90 s association step, followed by a 240 s dissociation in running buffer. A 90 s pulse of 100 mM HCl was applied to regenerate the surface at the end of each cycle. A pentadecapeptide, A15scr, containing the constituient amino acids of A15 in a random sequence (H-RAGTATTLADLHYST-NH_2) was injected under the same conditions as a control for instrument artifacts such as refractive index changes and non-specific binding.

2.3. Data analysis

Biosensor data were prepared, modelled and fitted by means of the BIAevaluation 3.0.1. software. Calculations are carried out by numerical integration [22] and global curve fitting is done by non-linear least-squares analysis [23] applied simultaneously to the entire data set [10,24]. The quality of the fitted data can be evaluated by comparison between the modeled and the experimental sensorgrams, as well as by statistical parameters such as the chi squared, given by Eq. (1), where r_f is the fitted value at a given point, r_x is the experimental value at the same point, n is the number of data points and p is the number of degrees of freedom.

$$\chi^2 = \frac{\sum_1^n (r_f - r_x)^2}{n - p} \quad (1)$$

The reaction models and correspondent differential rate equations tested are presented in Table 1.

Table 1
Reaction schemes and differential rate equations tested. Symbols are described in nomenclature. Subscripts 1 and 2 refer to the parallel binding events in two different ligand subpopulations

One-to-one reaction:
$A + L \Leftrightarrow AL$
$dR/dt = k_a C_A(R_{max} - R) - k_d R$
Parallel reactions (ligand heterogeneity):
$A + L_1 \Leftrightarrow AL_1$
$A + L_2 \Leftrightarrow AL_2$
$dR_1/dt = k_{a1} C_A(R_{max1} - R) - k_{d1} R$
$dR_2/dt = k_{a2} C_A(R_{max2} - R) - k_{d2} R$

3. Results and discussion

3.1. Optimization of the experimental setup

In our first approach, we tried to overcome the detection problems to be expected from the low molecular weight (MW) of our analytes by using a very dense SD6 surface (8 ng/mm^2) and high peptide concentrations at a low flow rate (5 μl/min). The sensorgrams generated under these conditions (Fig. 1a) could not be fitted to the 1:1 bimolecular model (Table 1) as inferred from the high and non-random residuals obtained (Fig. 1b) and from the fact that the association rate constant was concentration-dependent (Fig. 1c). Fitting the data to the heterogeneous ligand model (Table 1), the residuals were lower and randomly distributed, but the values for k_{a1} and k_{a2} were still concentration-dependent (data not shown). Since previous X-ray diffraction crystallographic studies have suggested that SD6 binds to FMDV C-S8c1 through a single Fab fragment [14,18], we expected a 1:1 SD6/A15 interaction. Therefore, the inconsistency of the kinetic data was attributed to the high SD6 density employed, which generated significant heterogeneity in ligand accessibility and orientation, as well as favoured diffusion-controlled delivery of analyte to the most hindered SD6 molecules [25]. Analysis of a broad range of A15 concentrations at the same flow rate but over less dense (1.7 and 0.8 ng/mm^2) SD6 surfaces did

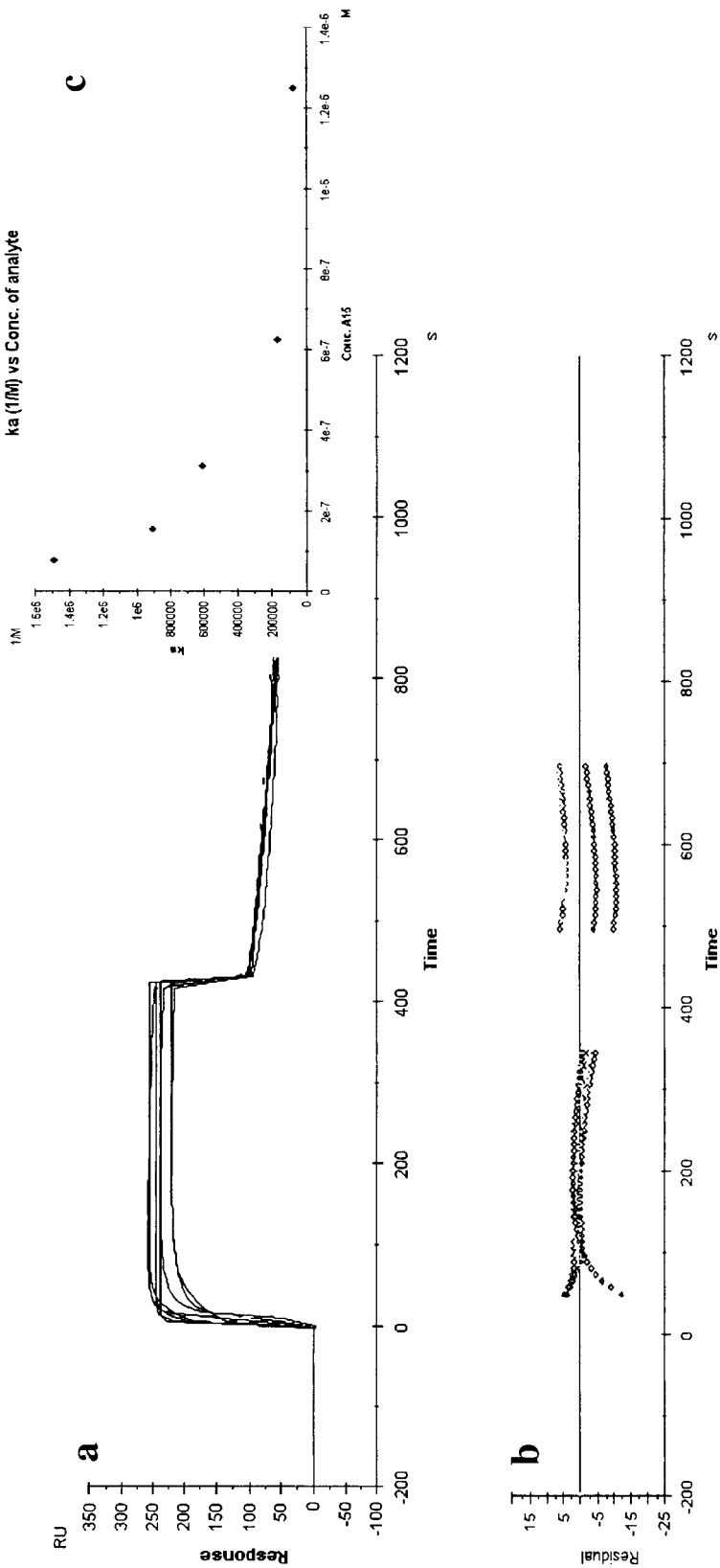

Fig. 1. Biosensor analysis of A15 injected over a 8 ng/mm^2 SD6 surface, at a 5 ml/min buffer flow rate: (a) sensorgrams (78, 156, 305, 610 and 1220 nM); (b) residuals (approximately ±12 RU); (c) dependence of k_a on analyte concentration.

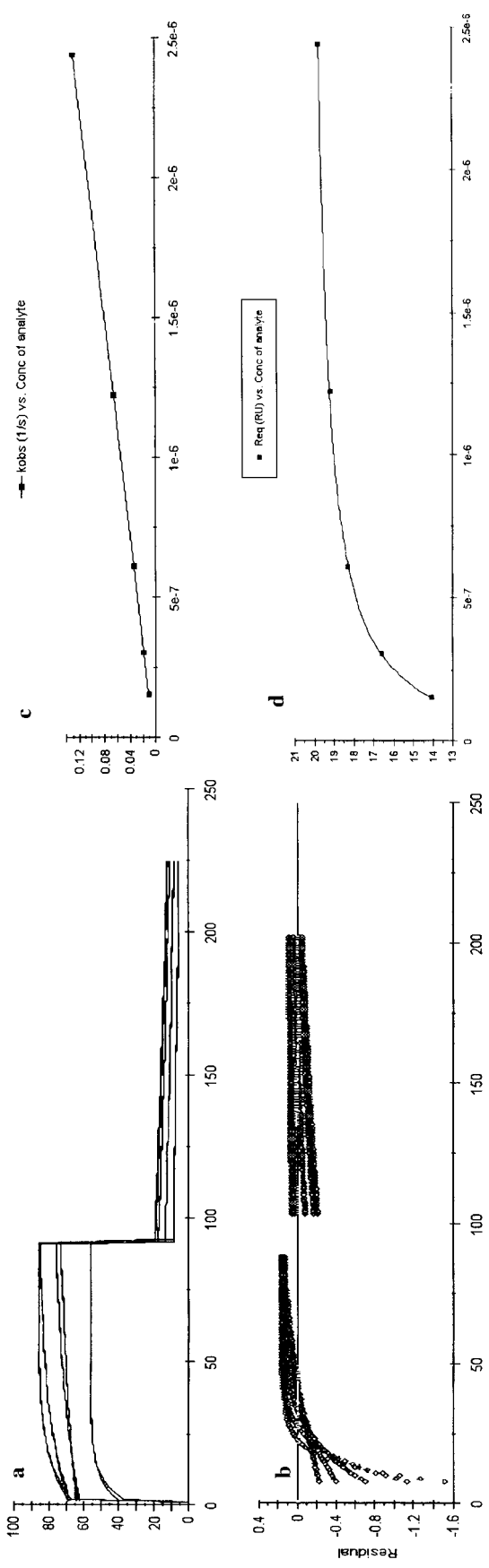

Fig. 2. Biosensor analysis of A15 injected over a 1.7 ng/mm^2 SD6 surface, at a 60 ml/min buffer flow rate: (a) sensorgrams (156, 305, 610, 1220 and 2440 nM); (b) residuals (approximately ±0.5 RU); (c) linearity of k_s on analyte concentration; (d) R_{eq} versus analyte concentration plot.

Table 2
Kinetic data of the interaction between MAb SD6 and 44 site A peptides, corrected for bulk effects (see text). Qualitative relative antigenicities obtained in ELISA competition assays [18] are represented, with a black box corresponding to $IC_{50} > 100$, a dark grey box to $IC_{50} = 30$ to 100, a light grey box to $IC_{50} = 5$ to 30 and a white box to $IC_{50} < 5$. no, no interaction; nr, non-reliable data

PEPTIDE	$k_a/M^{-1}s^{-1}$	k_d/s^{-1}	K_A/M^{-1}	ELISA
A15	$7.27x10^4$	$1.36x10^{-3}$	$5.36x10^7$	
A15(137P)	$5.83x10^4$	$1.86x10^{-3}$	$3.14x10^7$	
A15(138P)	no	no	no	
A15(139P)	no	no	no	
A15(140P)	$7.39x10^4$	$2.10x10^{-3}$	$3.51x10^7$	
A15(141P)	no	no	no	
A15(142P)	no	no	no	
A15(143P)	no	no	no	
A15(144P)	no	no	no	
A15(145P)	no	no	no	
A15(146P)	no	no	no	
A15(147P)	no	no	no	
A15(148P)	$6.65x10^4$	$6.21x10^{-2}$	$1.07x10^7$	
A15(137S)	$1.22x10^5$	$3.50x10^{-3}$	$3.50x10^7$	
A15(138S)	$1.09x10^5$	$1.23x10^{-2}$	$8.84x10^6$	
A15(140S)	$1.51x10^5$	$8.63x10^{-4}$	$1.75x10^8$	
A15(141S)	nr	nr	nr	
A15(142S)	$4.31x10^4$	$5.59x10^{-3}$	$1.10x10^7$	
A15(143S)	no	no	no	
A15(144S)	no	no	no	
A15(145S)	$4.01x10^4$	$5.11x10^{-3}$	$7.84x10^6$	
A15(147S)	$1.27x10^4$	$1.10x10^{-2}$	$1.15x10^7$	

PEPTIDE	$k_a/M^{-1}s^{-1}$	k_d/s^{-1}	K_A/M^{-1}	ELISA
A15(148S)	$9.42x10^4$	$6.71x10^{-3}$	$1.40x10^7$	
A15(138D)	no	no	no	
A15(138E)	no	no	no	
A15(138F)	$8.62x10^4$	$3.86x10^{-3}$	$2.23x10^7$	
A15(138K)	no	no	no	
A15(138R)	no	no	no	
A15(138V)	$1.32x10^5$	$7.12x10^{-3}$	$1.85x10^7$	
A15(138Y)	$2.29x10^5$	$8.81x10^{-3}$	$2.60x10^7$	
A15(145D)	no	no	no	
A15(145E)	$7.64x10^4$	$8.41x10^{-4}$	$9.08x10^7$	
A15(145F)	no	no	no	
A15(145I)	no	no	no	
A15(145K)	$2.98x10^4$	$2.70x10^{-3}$	$1.10x10^7$	
A15(145R)	$3.54x10^4$	$2.40x10^{-3}$	$1.47x10^7$	
A15(147A)	$9.25x10^4$	$2.09x10^{-3}$	$4.43x10^7$	
A15(147D)	no	no	no	
A15(147E)	$6.66x10^4$	$3.07x10^{-3}$	$2.17x10^7$	
A15(147G)	$3.23x10^5$	$6.07x10^{-3}$	$3.72x10^7$	
A15(147K)	$6.56x10^4$	$3.37x10^{-3}$	$1.95x10^7$	
A15(147N)	$4.60x10^4$	$4.99x10^{-3}$	$9.21x10^6$	
A15(147R)	$7.88x10^4$	$3.49x10^{-3}$	$2.26x10^7$	
A15(147V)	$9.24x10^4$	$6.65x10^{-3}$	$1.39x10^7$	

not improve the results, the former surface producing equally inconsistent data and the latter being useless given the extremely low signal-to-noise ratios (data not shown).

Therefore, and using again a medium-density SD6 surface (1.7 ng/mm^2) and high peptide concentrations (150 to 2440 nM), we decided to increase the buffer flow rate up to 60 μl/min to obviate the diffusion-controlled kinetics which seemed the most probable source for the persisting deviations from the expected Langmuirian behaviour. Indeed, consistent and apparently reliable data were now obtained, with a random distribution of residuals within an interval of ca. ±0.5 RU, except for injection plugs (Fig. 2b). Linearity of k_s *versus* peptide concentration (Eq. (2)) over the 32-fold concentration range was observed, thus k_a was concentration independent (Fig. 2c).

$$k_s = k_a \times C_A + k_d \quad (2)$$

Modeled and experimental curves were virtually superimposable (Fig. 2a) and a χ^2 smaller than 1 was obtained. Data self-consistency was further confirmed by the total agreement between the values for the equilibrium association constant, K_A, as obtained from the k_a/k_d ratio or from the plot of R_{eq} versus peptide concentration (Eq. (3), Fig. 2d) for a 1:1 interaction. From this same plot, a value of R_{max} close to that predicted from the immobilization response, R_{immob} (Eq. (4)) was obtained, thus indicating that the MAb was fully active.

$$R_{eq} = \frac{K_A \times C_A \times R_{max}}{K_A \times C_A + 1} \quad (3)$$

$$R_{max} = R_{immob} \times \frac{MW_L}{MW_A} \quad (4)$$

3.2. Systematic analysis of site A peptides

Having found suitable experimental conditions for the kinetic analysis of the A15/SD6 interaction, we applied a similar protocol to the systematic screening of 43 other A15 analogues. Reduction of 'kinjection' times (90 s for association, 240 s for dissociation) lowered sample, buffer and time consumption, with no loss in sensorgram quality or kinetic information. The consistency and accuracy of the fitted kinetic data obtained for the whole set of site A peptides were in every aspect similar to those described for A15 under the same conditions. The stability of SD6 surfaces to the repeated acidic regeneration cycles allowed us to screen the entire set over the same surface, without any detectable loss in MAb activity, thus providing reliable comparison among the different peptides.

The scrambled 15-mer sequence A15Scr had no apparent specific binding, but gave rise to a high bulk response, as observed for the other peptides analysed. Therefore, the curves obtained for each site A peptide were corrected by subtraction of the corresponding A15Scr sensorgrams. A discrete overall improvement in data quality (lower χ^2 values) accompanied this correction and a general increase in K_A was obtained. This affinity increase reflected simultaneously an increase in k_a and a k_d decrease (data not shown). These findings are consistent with the higher probability of analyte non-specific retention within the dextran matrix when high concentrations are used [8,27]. This binding was probably a 'response averaging' of the biospecific union with the non-specific analyte imprisonment. The corrected biosensor data for the 44 site A peptides analysed are shown in Table 2, in which relative antigenicities derived from ELISA [18] are also represented. The general agreement observed between both techniques validates our analytical method for the antigenicity screening of low MW peptides using biosensor technology.

4. Concluding remarks

This investigation has served three major purposes:

1. It shows that BIAcore technology is a powerful tool to monitor and characterize antigen–antibody interactions even when low MW analytes are used. This provides a new basis for fast and straightforward antigenicity ranking of small synthetic peptide antigens.
2. It emphasizes the need for careful experimental setup and optimization to obviate the problems usually found in quantitative kinetic biosensor analysis.
3. It demonstrates the correspondence between peptide–antibody affinities as obtained by BIAcore or ELISA experiments.

Although evanescent wave biosensors are successful [1–9] in that they provide simple and fast ('yes' or 'no') answers about the binding of analytes to a ligand, the quantitative data obtained from them are subject to several potential artifacts [7,8,25–28]. The most common sources for such artifacts are heterogeneity in ligand accessibility and orientation, as well as mass-transport limitations. Methods for diagnosis and evaluation of these artifacts, such as global analysis of data sets generated in different surface capacities or self-consistency tests, are extensively discussed in the literature [24–32]. Nevertheless, these control tests, though helpful to ensure internally consistent data, provide no critical information about the validity of the kinetic parameters as absolute values. We minimized the undesired artifacts by adapting our experimental setup to high buffer flow rate and the minimum surface capacity possible and thus obtained self-consistent kinetic and equilibrium data, further confirmed by previous ELISA experiments [18].

However, caution is still advisable in the evaluation of such kinetic data. Firstly, one cannot totally compare the events taking place in a biosensor experiment with those occurring in physiologic media. It must not be forgotten that although no labels are required in biosensor analysis, the ligand is still somehow 'labelled' by its attachment to a sensor chip. Secondly, while ELISA provides a valuable check of the reliability of biosensor data, one cannot write off the possibility that mass-transport affects actual k_a and k_d values by a similar factor, thus providing thermodynamic constants apparently consistent with equilibrium experiments. In fact, a preliminary analysis of the A15/SD6 interaction using IAsys biosensor (a resonant mirror evanescent wave biosensor where a stirred cuvette, instead of a flowcell, is claimed to overcome mass-transport limitations) showed virtually the same affinity constant but slightly higher kinetic rate constants [33].

Further experiments in progress include using other anti-site A MAbs as ligands and a high MW analyte (a 1:1 conjugate of A15 with a carrier protein) for real-time competitive analysis [20]. These experiments will hopefully provide further information on the validity of our methodology.

Acknowledgements

We thank Dr. Maria Luz Valero for supplying the synthetic pentadecapeptides, Dr. Esteban Domingo and Dr. Mauricio Mateu (CBM-CSIC, Madrid) for the ELISA competition experiments and Dr. Nuria

Verdaguer for supplying the MAb SD6. We are grateful to the Scientific-Technical Services of the University of Barcelona for providing the BIAcore 1000 instrument, BIAevaluation 3.0.1 software and all the BIAcertified reagents and materials. Work supported by grants from the European Union (FAIR PL97-3577), DGICYT (Spain, grants PB94-0845 and PB97-0873) and Generalitat de Catalunya (CERBA). P.G. thanks the Fundaçao Calouste Gulbenkian (Lisbon, Portugal) for her Ph.D. grant and the Oporto University (Portugal) for a temporary leave from teaching duties.

References

[1] Fagerstam LG, Frostell-Karlsson A, Karlsson R, Persson B, Ronnberg I. Biospecific interaction analysis using SPR detection applied to kinetic binding site and concentration analysis. J Chromatogr 1992;597:397–410.

[2] Brigham-Burke M, Edwards JR, O'Shannessy DJ. Detection of receptor–ligand interactions using SPR: model studies employing the HIV-1 gp120/CD4 interaction. Anal Biochem 1992;205:125–31.

[3] Altschuh D, Dubs MC, Weiss E, Zeder-Lutz G, Van Regenmortel MHV. Determination of kinetic constants for the interaction between a monoclonal antibody and peptides using SPR. Biochemistry 1992;31:6298–304.

[4] Van Regenmortel MHV, Altschuh D, Pellequer JL, Richalet-Sécordel P, Saunal H, Wiley JA, Zeder-Lutz G. Analysis of viral antigens using biosensor technology. Methods Comp Methods Enzymol 1994;6:177–87.

[5] Lasonder E, Schellekens GA, Koedijk DGAM, Damhof RA, Welling-Wester S, Feijlbrief M, Scheffer AJ, Welling GW. Kinetic analysis of synthetic analogues of linear-epitope peptides of glycoprotein D of herpes simplex virus type I by SPR. Eur J Biochem 1996;240:209–14.

[6] Zeder-Lutz G, Zuber E, Witz J, Van Regenmortel MHV. Thermodynamic analysis of antigen–antibody binding using biosensor measurements at different temperatures. Anal Biochem 1997;246:123–32.

[7] Schuck P. Use of SPR resonance to probe the equilibrium and dynamic aspects of interactions between biological macromolecules. Ann Rev Biophys Biomol Struct 1997;26:541–66.

[8] Garland PB. Optical evanescent wave methods for the study of biomolecular interactions. Q Rev Biophys 1996;29(1):91–117.

[9] Lakey JH, Ragget EM. Measuring protein–protein interactions. Curr Opin Struct Biol 1998;8:119–23.

[10] Malmqvist M, Karlsson R. Biomolecular interaction analysis: affinity biosensor technologies for functional analysis of proteins. Curr Opin Chem Biol 1997;1:378–83.

[11] Lofas S, Johnsson B. A novel hydrogel matrix on gold surface in SPR sensors for fast and efficient covalent immobilization of ligands. J Chem Soc Chem Commun 1990;1526–1528.

[12] Johnsson B, Lofas S, Lindquist G. Immobilization of proteins to a carboxylmethyl dextran modified gold surface for biospecific interaction analysis in SPR sensors. Anal Biochem 1991;198:268–77.

[13] Carreño C, Roig X, Cairó J, Camarero J, Mateu MG, Domingo E, Giralt E, Andreu D. Studies on antigenic variability of C strains of FMDV by means of synthetic peptides and monoclonal antibodies. Int J Peptide Protein Res 1992;39:41–7.

[14] Verdaguer N, Mateu MG, Andreu D, Giralt E, Domingo E, Fita I. Structure of the major antigenic loop of FMDV complexed with a neutralizing antibody: direct involvement of the Arg–Gly–Asp motif in the interaction. EMBO J 1995;14(8):1690–6.

[15] Mateu MG, Camarero JA, Giralt E, Andreu D, Domingo E. Direct evaluation of the immunodominance of a major antigenic site of FMDV in a natural host. Virology 1995;206:298–306.

[16] Feigelstock DA, Mateu MG, Valero ML, Andreu D, Domingo E, Palma EL. Emerging FMDV variants with antigenically critical amino acid substitutions predicted by model studies using reference viruses. Vaccine 1996;14(2):97–102.

[17] Mateu MG, Valero ML, Andreu D, Domingo E. Systematic replacement of amino acid residues within an Arg–Gly–Asp-containing loop of FMDV and effect on cell recognition. J Biol Chem 1996;271(22):12814–9.

[18] Verdaguer N, Sevilla N, Valero ML, Stuart D, Brocchi E, Andreu D, Giralt E, Domingo E, Mateu MG, Fita I. A similar pattern of interaction for different antibodies with a major antigenic site of FMDV: implications for intratypic antigenic variation. J Virol 1998;72(1):739–48.

[19] Domingo E, Mateu MG, Martínez MA, Dopazo J, Moya A, Sobrino F. Genetic variability and antigenic diversity of foot-and-mouth disease virus. In: Kurstak K, Marusyk RG, Van Regenmortel MHV, editors. Applied Virology Research, vol. 2. Plenum Publishing Corporation. 1990. p. 233–265.

[20] Karlsson R. Real-time competitive kinetic analysis of interactions between low-molecular-weight ligands in solution and surface-immobilized receptors. Anal Biochem 1994;221:142–51.

[21] Karlsson R, Stahlberg R. SPR detection and multispot sensing for direct monitoring of interactions involving low-molecular-weight analytes and for determination of low affinities. Anal Biochem 1995;228:274–80.

[22] Morton TA, Myszka DG, Chaiken IM. Interpreting complex binding kinetics from optical biosensors: a comparison of analysis by linearization, the integrated rate equation and numerical integration. Anal Biochem 1995;227:176–85.

[23] O'Shannessy DJ, Brigham-Burke M, Soneson KK, Hensley P, Brookes I. Determination of rate and equilibrium binding constants for macromolecular interactions using SPR: use of non-linear least squares analysis methods. Anal Biochem 1993;212:457–68.

[24] Karlsson R, Falt A. Experimental design for kinetic analysis of protein–protein interactions with SPR biosensors. J Immunol Methods 1997;200:121–33.

[25] O'Shannessy DJ, Winzor DJ. Interpretation of deviations from pseudo-first-order kinetic behavior in the characterization of ligand binding by biosensor technology. Anal Biochem 1996;236:275–83.

[26] Hall DR, Cann JR, Winzor DJ. Demonstration of an upper limit to the range of association rate constants amenable to study by biosensor technology based on SPR. Anal Biochem 1996;235:175–84.

[27] Schuck P, Minton AP. Analysis of mass transport-limited binding kinetics in evanescent wave biosensors. Anal Biochem 1996;240:262–72.

[28] Oddie GW, Gruen LC, Odgers GA, King LG, Kortt AA. Identification and minimization of non-ideal binding effects in BIAcore analysis: ferritin/anti-ferritin Fab′ interaction as a model system. Anal Biochem 1997;244:301–11.

[29] Bowles MR, Hall DR, Pond SM, Winzor DJ. Studies of protein interactions by biosensor technology: an alternative approach to the analysis of sensorgrams deviating from pseudo-first-order kinetic behavior. Anal Biochem 1997;244:133–43.

[30] Edwards PR, Leatherbarrow RJ. Determination of association rate constants by an optical biosensor using initial rate analysis. Anal Biochem 1997;246:1–6.

[31] Myszka DG, Morton TA, Doyle ML, Chaiken IM. Kinetic

analysis of a protein–antigen interaction limited by mass transport on an optical biosensor. Biophys Chem 1997;64:127–37.
[32] Schuck P, Minton AP. Kinetic analysis of biosensor data: elementary tests for auto-consistency. Trends in Biochem Sci 1996;21:458–60.
[33] Gomes P, Giralt E, Andreu D, unpublished results.